TMotion: Embedded 3D Mobile Input using Magnetic Sensing Technique

Sang Ho Yoon, Ke Huo, Karthik Ramani
School of Mechanical Engineering
Purdue University, West Lafayette, IN, USA
{yoon87, khuo, ramani}@purdue.edu

ABSTRACT
We present TMotion, a self-contained 3D input that enables spatial interactions around mobile device using a magnetic sensing technique. We embed a permanent magnet and an inertial measurement unit (IMU) in a stylus. When the stylus moves around the mobile device, we obtain a continuous magnetometer readings. By numerically solving non-linear magnetic field equations with known orientation from IMU, we achieve 3D position tracking with update rate greater than 30Hz. Our experiments evaluated the position tracking accuracy, showing an average error of 4.55mm in the space of 80mm×120mm×100mm. Furthermore, the experiments confirmed the tracking robustness against orientations and dynamic tracings. In task evaluations, we verified the tracking and targeting performance in spatial interactions with users. We demonstrate example applications that highlight TMotion's interaction capability.

Figure 1. TMotion enables a real-time 3D position tracking using embedded permanent magnet and IMU with existing mobile device. TMotion provides interaction spaces above and behind the device while supporting discrete and continuous interactions.

ACM Classification Keywords
H.5.2. [Information Interfaces and Presentation]: User Interfaces. – Input devices and strategies

Author Keywords
3D Input; Embedded Interaction; Sensing Technique; Mobile Interaction; Sensor Fusion; Around Device Interaction

INTRODUCTION
Recent developments in smartphone displays and sensors have resulted in enhanced visual experiences such as mobile augmented (AR) and virtual reality (VR) [10, 22]. To support these 3D interfaces, previous study suggested on providing a natural correspondence like human motion in 3D space from the input device [12]. 3D input method also offers more intuitive and quicker way to interact with 3D interfaces [25]. To this extent, researchers have proposed an around-device mobile interaction [6]. It frees a physical boundary limited by mobile device screens and incorporates surrounding 3D space as an interaction space. Recent works employ 2D tracking [13] and event-based discrete inputs [15] in 3D space to enlarge the interaction space. Inspired from these works, we develop a real-time 3D position tracking technique, which enables rich spatial mobile input.

Acquiring input data from 3D mobile space has been investigated through vision and magnet-based techniques. Recent work shows mid-air gesture-based interaction using a depth camera [9]. Occlusion and lighting condition still limit the use of vision-based techniques in mobile environments. On the other hand, the magnetic sensing techniques which are free from occlusion and different light conditions have also been investigated [8, 19]. Although these works show high 2D/3D tracking accuracy in real-time operation, they still require either a desktop computation, or extensive modifications on the mobile device.

In our work, TMotion enables the mobile device to track a stylus embedded with a magnet and an IMU. Specifically, the algorithm calculates the magnet's position relative to the mobile based on the magnetic field vector and the orientation of the embedded magnet. We achieve a 3D position tracking rate greater than 30Hz possibly with mobile device. As a 3D mobile input, TMotion supports continuous/discontinuous interactions in above/behind device spaces. Our contributions include the following:

- A novel sensing technique providing a real-time position tracking as 3D mobile input

TEI '16, February 14-17, 2016, Eindhoven, Netherlands
© 2016 ACM. ISBN 978-1-4503-3582-9/16/02...$15.00
DOI: http://dx.doi.org/10.1145/2839462.2839463

- An analysis of experiments and task evaluations including tracking and targeting accuracy using TMotion
- Demonstration of example applications exploring embedded continuous/discrete interactions in expanded spaces.

RELATED WORK

TMotion draws its inspiration from around-device interaction, position tracking using magnetic sensing technique, and embedded interface with smart stylus. We describe key works in these fields that formulate our work.

Around Device Interaction

Around-device interaction using 3D space has been explored with different set of sensing techniques while achieving equivalent performance with touch input [16]. Optical and vision based sensing techniques including depth cameras, IR proximity, and RGB camera are exploited to augment the general interaction with mobile device [9, 6, 27]. However, these techniques require on the line-of-sight view of hand/interaction medium which limit the interaction space within the range of camera or optical sensor. In our work, we adopt a magnetic sensing technique to encompass a full 3D volume around the mobile device.

Around-device interaction with magnetic sensing has been investigated. Abracadabra and Nenya demonstrated 1D and 2D tracking techniques based on a single magnetometer to showcase the potential of magnet sensing as an input metaphor [2, 13]. In a similar manner, later works introduce the use of magnetic sensing to achieve delicate and rich mobile interactions [4, 7, 15, 17]. However, these works still focus on retrieving discrete gesture inputs or 2D position tracking for symbolic interactions. We focus on embedding 3D tracking through which user's embodied motions are projected into intended interaction directly.

Position Tracking Using Magnetic Sensing Technique

Magnetic sensing has been explored extensively for position tracking. Polhemus and Sixense both provide highly accurate 3D position tracking system in a large space [18, 23]. However, these approaches use an active magnetic source which requires the user to stay within the range of set-up space, thus not applicable for mobile usage scenario. To address this issue while supporting collaborative setting, recent works investigate on tracking multiple magnetic tokens using electromagnets [31] and spinning permanent magnets [4]. Although their methods support tracking of multiple tokens, our approach focuses on providing precise 3D tracking to augment around device interaction for a single user.

Passive magnetic source has been adopted to accomplish 3D mobile input. GaussSense provides a magnet tracking system with 192 Hall-effect sensors embedded board [19]. However, the sensor board should be installed at the back of the device and only supports near-surface tracking (within 20mm). uTrack implements 3D position tracking of a permanent magnet using two magnetometers. It supports an accurate 3D inputs for wearables application [8]. As discussed by the authors, however, it still requires a desktop computation due to the extensive search algorithm. The heavy computation limits scalability and practicability as a stand-alone input technique for the mobile device. TMotion provides a real-time tracking with a larger interaction volume solely based on the existing components of the mobile device.

Embedded Interface with Smart Stylus

Emerging smartphone, tablet and laptop equipped with smart styli enabling new input metaphors [20, 24]. Different aspects of the stylus have been studied including palm rejection [1], grip-based input [26], cross-device interaction [14], and high-resolution pressure sensing [21]. These approaches focus on either improving the digital pen experience more toward pen & paper interaction or enhancing the 2D user interface. On the other hand, we develop spatial and physical interactions enabled by our technique to expand the interaction space by providing 3D tracking. Respectively, we demonstrate applications where users perform discrete/continuous interactions in above/behind device spaces.

POSITION TRACKING PRINCIPLE & ALGORITHM

2D and 3D position tracking using multiple magnetic sensors have been explored [8, 11, 19]. However, they require either hardware modification or desktop computation. In this section, we introduce the background knowledge of the magnetic field sensing and our novel approach.

From the magnetism theory, 3D position of the permanent magnet in the magnetic sensor oriented space ($\mathcal{F}_{mobile}$) can be solved using the following equation

$$\mathbf{H}(\mathbf{r}) = \frac{K}{r^3}\left[\frac{3\mathbf{r}(\mathbf{m}\cdot\mathbf{r})}{r^2} - m\right], r = |\mathbf{r}|, K = \frac{M}{4\pi} \quad (1)$$

Here, H refers to the magnetic field vectors, M denotes for the magnetic moment, **m** is the directional vector of the magnet, and **r** is the location vector of magnet relative to the sensor. With known **m**, M, and H, **r** can be solved.

We assume magnet is located at (x, y, z) resulting in **r** to be $(-x, -y, -z)$. The directional unit vector of magnet

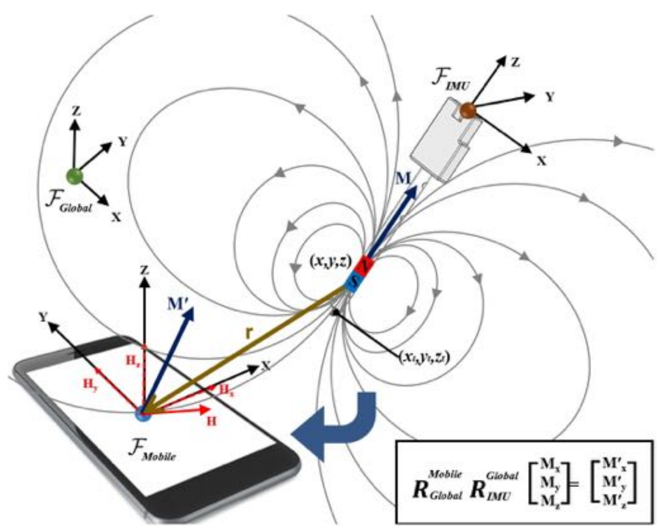

Figure 2. Magnetic vector (H) is generated by magnet. Magnetic directional vector from TMotion (M) is transformed to mobile's frame (M').

is ($\mathbf{M}_x$,$\mathbf{M}_y$,$\mathbf{M}_z$). We perform space transformation from IMU space ($\mathcal{F}_{IMU}$) to mobile space ($\mathcal{F}_{mobile}$). Figure 2 illustrates the transformation of the directional unit vectors ($\mathbf{M}$) from TMotion to the mobile space ($\mathbf{M}'$). Thus, Eq. (1) can be dissected into the following three scalar nonlinear equations.

$$\mathbf{H}_x = \frac{K}{(x^2+y^2+z^2)^{\frac{5}{2}}}\left[-3x(-M'_x x - M'_y y - M'_z z) - M'_x(x^2+y^2+z^2)\right]$$
$$\mathbf{H}_y = \frac{K}{(x^2+y^2+z^2)^{\frac{5}{2}}}\left[-3y(-M'_x x - M'_y y - M'_z z) - M'_y(x^2+y^2+z^2)\right]$$
$$\mathbf{H}_z = \frac{K}{(x^2+y^2+z^2)^{\frac{5}{2}}}\left[-3z(-M'_x x - M'_y y - M'_z z) - M'_z(x^2+y^2+z^2)\right] \quad (2)$$

$$[J(x^{(n)})v^{(n)}] = -F(x^{(n)}), \quad e = 10^{-7} \quad (3)$$

$$\begin{bmatrix} x_t \\ y_t \\ z_t \end{bmatrix} = \begin{bmatrix} x \\ y \\ z \end{bmatrix} + R^{Mobile}_{Global} R^{Global}_{IMU} T^{Magnet}_{Tip} \quad (4)$$

By taking known orientations from attached IMU ($\mathbf{M}$) and 3-axis magnetometer readings ($\mathbf{H}$) from a mobile device as inputs, we employ Newton's method (Eq. 3) to solve nonlinear Eq. 2. Figure 3 illustrates the system flow of our technique:

1. Input orientations from IMU ($\mathbf{M}$) and magnetometer readings from phone's magnetometer ($\mathbf{H}$) to the system.
2. Apply space transformation to calculate orientation ($\mathbf{M}'$) in the mobile space ($\mathcal{F}_{mobile}$)
3. Apply Newton's Method to solve nonlinear equations (Eq. 2). If it fails to converge ($e{<}10^{-7}$) within 15 iterations (i) or diverges ($e{>}10^3$) at any time, returns to the beginning to process new input signals.
4. On successful computation, updates an initial value with a new root (x, y, z) and apply transformation (Eq. 4) to the root (x, y, z) for deriving the tip position (x_t, y_t, z_t).

Our approach enables a faster computation since we conduct the numerical solving once with known orientations from IMU. Whereas [8] requires multiple iterations of solving equations for the exhaustive searching. In preliminary work, we observe that the position tracking succeeds when the prototype operates within 160mm × 160mm × 200mm volume around the mobile device. The limited sensing range is due to the fact that the magnet strength is inversely proportional to the cubic distance to the magnetometer. Newton's method fails to converge occasionally due to mismatched pair of inputs (IMU orientation & mobile's magnetometer reading). The mismatches are potentially caused by the low signal to noise ratio when the permanent magnet locates at the tracking range borderline. To compensate this issue, we simply apply thresholding to pass valid sensor readings to the numerical solver. With the mitigation, we do not observe computation failure during continuous motion within the interaction volume.

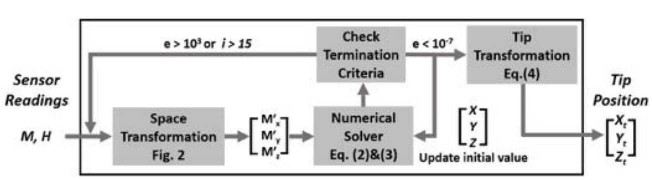

Figure 3. Tracking algorithm finds magnet's position through numerical solver and performs transformation to output the tip position. With known orientations, exhaustive search is not required.

In our work, we adopt a 9 degrees-of-freedom (DOF) IMU to disambiguate the unknown orientations which enables real-time mobile 3D tracking using a single magnetometer. Thus, we achieve a stand-alone mobile input which performs in a real-time and can be used with an unmodified mobile device. This approach distinguishes us from related works [8, 19].

IMPLEMENTATION

Figure 4 illustrates our prototype in detail. The diameter and the length of the prototype are 10mm and 170mm respectively. The prototype can hold multiple form factors to support embedded magnets of various orientation and size. While the stylus form is assumed to offer better comfort on and above device interaction, the wand design is considered to provide better comfort for behind device interaction. The conductive rubber is placed at the stylus tip to support conventional touch input. In our demonstration, we use a cylinder-shaped, N42 grade, neodymium magnet with 3.2x11mm in diameter and length respectively.

Hardware

For orientation, we use Sparkfun's 9DOF sensor stick which comprises of gyroscope (*Invensense ITG-3200*), magnetometer (*Honeywell HMC5883L*), and accelerometer (*Analog Devices ADXL345*). These sensors meet the technical requirement including sensing range and resolution. To avoid the magnetometer saturation, we configure the sensor stick and the embedded magnet in distinct locations (>5cm) in our prototype. Furthermore, we adopt an one-time calibration including scaling each axis value relative to the gravity (accelerometer), subtracting offset reading (gyroscope) and soft+hard iron calibration (magnetometer) [5]. The initial calibration process ensures the functionality of the IMU regardless of the embedded permanent magnet. The micro-controller integrated with a Bluetooth 4.0 Low Energy (BLE) module (ATmega32U4, Nordic nRF8001) captures and transmits analog readings from sensors to the smartphone wirelessly. We use a 110mAh battery which provides 6 hours of

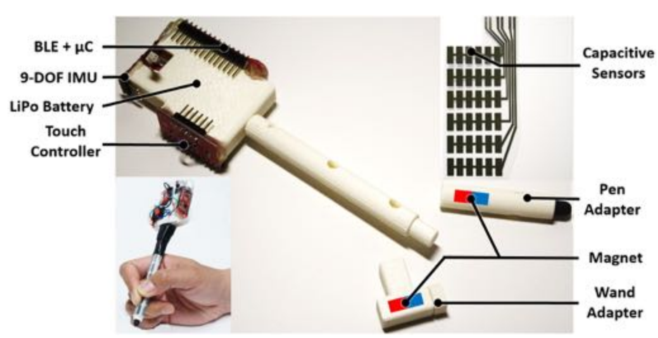

Figure 4. TMotion prototype and breakdown of its components. Permanent magnet and 9DOF-IMU are embedded for 3D position tracking.

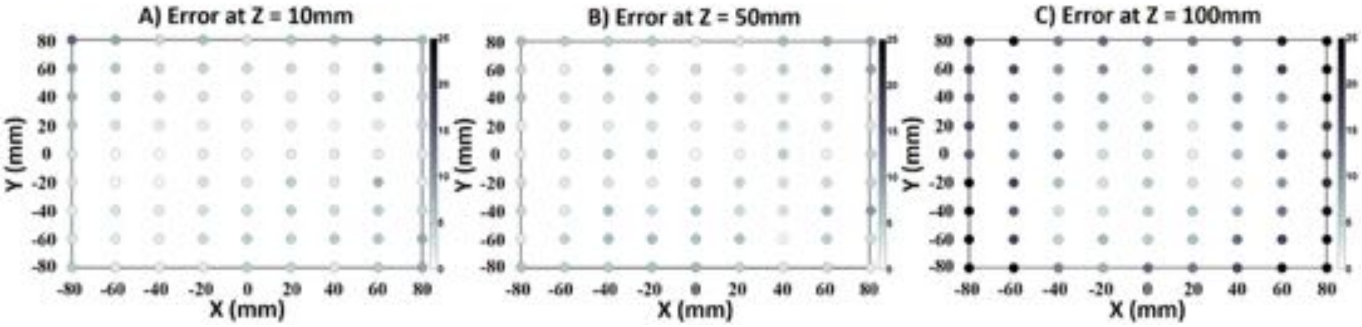

Figure 5. Tracking accuracy is tested in three heights a) 10mm, b) 50mm, and c) 100mm using TMotion. The grayscale indicates the Euclidean distance between the ground truth and our tracking. Origin of the graph represents the center of the magnetometer from mobile device's side. The mean error is 4.55mm in the volume that covers the 5.5′′ smartphone, 80mm (x-axis) × 120mm (y-axis) × 100mm (z-axis)

active operation with peak performance. For capacitive sensing, we inkjet-printed a sheet of electrodes using *AgIC* ink while processing capacitive proximity through *MPR121*.

We formed a self-contained setup using *LG Optimus G Pro* smartphone (1.7GHz quad-core with 2GB RAM). We were unable to retrieve the location of the embedded magnetometer from vendor's manual, and that necessitates an additional magnetometer attachment on the mobile. Here, we added a single *HMC5883L* with a microcontroller at the back of the phone using On-The-Go cable. Evidently, given the accurate sensor placement information of the mobile device, we need no such modification.

Software

The orientation of the prototype is computed using Direction Cosine Matrix algorithm for fast and stable performance during dynamic motion. The microcontroller streams calculated Euler angles and capacitive touch sensor values (15 bytes in total) through the BLE module (45∼50Hz). With the streamed mobile's magnetometer data (75Hz), we update the tip position from the latest computation. In our test setup, each numerical computation takes between 1∼8ms (3ms in average), which results in overall tracking rate of >30Hz. In the example applications, we adopted Kalman filter to smooth the raw data. For capacitive sensing, we set threshold value to detect the tap gesture. The system requires an initial calibration to compensate noises from the geomagnetic field. We subtract average magnetometer readings before the prototype gets into the interaction volume.

TRACKING ACCURACY EXPERIMENT

To find out the tracking performance of TMotion, we have conducted three experiments: tracking accuracy in different 1) heights, 2) orientations, and 3) tracings. We measured accuracy performance by comparing Euclidean distance between a physical ground truth and computed positions. We set a plastic shelf (160mm×160mm) covered with a grid paper (20mm space in both x and y directions). We adjusted the height of the shelf with a set of blocks to test the prototype in heights of 10, 50, and 100mm above the mobile device. We placed the prototype's tip on each grid intersection point with normal usage orientations (0∼60°) and recorded 100 readings at each point. The overall testing volume was 160mm (x-axis), 160mm (y-axis), and 10∼100mm (z-axis) about the magnetometer's center, with a total number of 24300 data points (100 readings x 81 intersections x 3 heights).

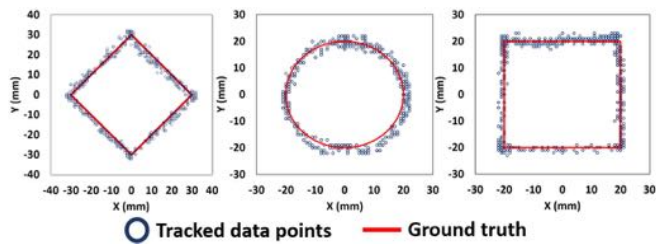

Figure 6. Visualization of the shape tracing at 50mm above the device.

To further investigate the effect of the different orientations, we rotated the prototype around a set of fixed points for (1) normal usage range (<60°) and (2) steeper tilt angles (60∼90°). A total of 5000 data points were captured at five fixed points [0,0],[-50,-50],[-50,50],[50,-50],[50,50] with z=50mm. At last, we traced the printed shapes on the testing jig which were assumed to be our ground truth. We repeatedly traced each shape for 40s and captured more than 1000 data points.

Results

Figure 5 illustrates the Euclidean distance between our readings and the ground truth at each point. In a total volume with 160mm(W)×160mm(H)×100mm(D), an average error is 6.27mm (σ = 4.56mm). The errors are mainly caused by the environmental magnetic field noises as the prototype moves away from the sensor similar to previous works [8, 13]. If we narrow down to an interaction space of 80mm(W)×120mm(H)×100mm(D) which still encapsulates the 5.5′′ smartphone, the error significantly reduces to the 4.55mm (σ = 2.6mm). It is also noticeable that the tracking shows more errors near the center at z = 10mm than at z = 50mm. Such inconsistency is caused by the saturated magnetometer readings when the magnet approaches the center at z = 10mm due to the strong magnet strength. For later task evaluations and applications, we adopt a height range of 10∼100mm as our interaction space.

We carried out experiments to test performance variations during different orientations and dynamic tracings. For normal usage orientation (<60°), the mean error was

Figure 7. Evaluation task setup: (a) given physical object for measurement, (b) participant measures length of the object (Task 1) and (c) Participant navigates along z-axis for targeting task (Task 2).

μ = 5.66mm (σ = 3.33mm). The steeper orientation (60°∼90°) showed no significant increase in the mean error (μ = 6.13mm, σ = 3.05mm). Thus, our tracking technique performs uniformly regardless of tilt angles. For tracing, we came up with a visual inspection of traced data points to confirm the dynamic performance of our tracking. As shown in Figure 6, the tracking performance does not degrade significantly comparing with previous results. The tracing results still form a shape similar to the ground truth and the z-direction tracking deviates within ±1.5mm.

TASK EVALUATIONS

For further verification of using TMotion as an embedded 3D mobile input, we conducted two task evaluations with the same test set-up from previous experiments. We carried out evaluation tasks to investigate the applicability and design guidelines for such 3D input. We recruited 14 participants (13 males, 1 female) with a mean age of 28. All participants had previous experience with smartphones over 3 years and one of them was left-handed. Participants were seated at the table throughout the study due to the duration of the evaluation. Users performed following tasks with TMotion.

Task1: Tracking accuracy during physical measurement

In Task 1, we evaluated the tracking accuracy when users interact with the physical object above the device. We conducted the task in a physical measurement scenario and that allows us to quantitatively analyze the performance of using TMotion. Participants were asked to perform length measurement on a provided object (Figure 7a) constructed with four skewed overhangs of different lengths (30mm and 50mm) and orientations (20°, 35°, 50°, and 75°). Participants were allowed to freely pose the object within the designated interaction space (80mm(W) x 120mm(H) x 100mm(D)) above the screen. Using capacitive sensing on the stylus body, users selected the start and end points along the overhang to complete one measurement (Figure 7b). Each measurement was repeated 5 times for a total of 40 trials for each user.

Table 1 shows average errors of measuring the given object using TMotion. The mean error for 50mm measurement is 1.67mm and 30mm measurement is 1.54mm. The error slightly increases for longer and steeper blocks due to the performance degradation at greater distance. Mean errors from participants show better accuracy than that of our tracking accuracy experiment (u = 4.55mm). This is mainly due to the fact that participant's natural habit to hold an object near the mobile device (0∼50mm). Furthermore, this observation

Length \ Angle	20^0	35^0	50^0	75^0	**Avg.**
30mm	0.77	1.34	2.03	2.01	**1.54**
50mm	1.56	1.45	1.59	2.09	**1.67**
Avg.	**1.16**	**1.40**	**1.81**	**2.05**	**1.61**

Table 1. Errors in measurements of using TMotion by users (in mm).

verifies the consistency of tracking performance while interacting with physical objects. We also want to highlight that users showed favors in the easiness of performing the spatial-tangible measurement in their feedbacks. All participants required less than 1 minute of training before the test.

Task2: Targeting accuracy above mobile device

In Task 2, we evaluated the participant's targeting controllability above the mobile device space with TMotion. The pointing task using finger and stylus showed similar performances in 2D scenario [3]. With regard to 3D interactions, recent work investigated on design guidance for finger input in mid-air space above the device [28]. From human ergonomic perspective, the result shows that 20mm is a minimum layer thickness necessary for targeting in the mid-air. Comparatively, our evaluation aims to verify whether the targeting performance using TMotion (stylus form) is similar to [28].

Participants were asked to navigate with the prototype above the device vertically regardless of horizontal direction and control given UI displaying user's cursor position as texts (Figure 7c). We asked users to select the randomly called layers with their elbows resting on the table. The qualifying criteria was to reach the called layer and stay reliably in it for 2 seconds. We set a height limit as 100mm above the screen and tested with 6 different layer thicknesses (50, 25, 20, 10, 5, and 2mm). Participants performed 20 trials on all 6 layer configurations. Additionally, we selected 20mm and 5mm as two representatives to perform elaborated studies (additional 80 trials for each).

As shown in Figure 8 (Left), the users achieve accuracy in excess of 98% with layer thickness of 20mm or greater. However, the accuracy drops with smaller layer thicknesses (<20mm) which is consistent with aforementioned finger point study [28]. Figure 8 (Right) shows the selection accuracy at different heights with 20mm and 5mm layer thickness. For the layers of 20mm thickness, the accuracy drops smoothly with increasing targeting height while

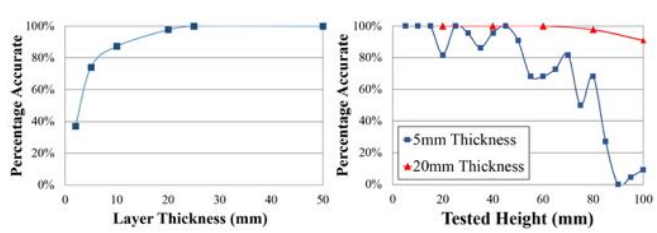

Figure 8. Left: Targeting accuracy with different layer thickness. Right: Targeting accuracy of 20mm and 5mm layer thickness at different heights above the mobile device

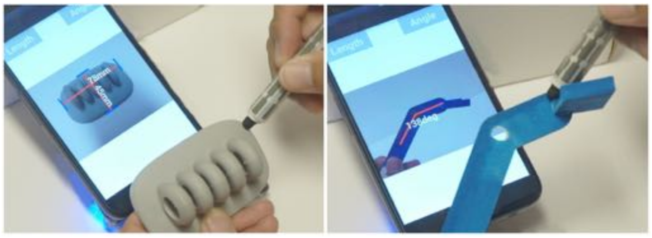

Figure 9. 3D position tracking guided by tap gesture enables physical measurements of length (Left) and angle (Right) above the device.

maintaining overall 98% accuracy. This is due to the degradation of system performance with larger distance from the magnetometer. With a 5mm layer thickness, however, we observe random pattern in accuracy drop. This is supported by comments from users where they report ergonomic issues like fatigues for precise control. In this task, it does not meet the perspective of Fitts' law since the system does not provide a uniform performance along different heights. With this result, we validate TMotion can serve as an alternative for finger input in above-device mid-air interaction space. Furthermore, this rationalizes employing the embodied mid-air input with TMotion as a promising discrete interaction metaphor.

EXAMPLE APPLICATIONS

To demonstrate the usage scenarios of our technique in around device interactions, we develop four applications. Enabled by the occlusion free 3D position tracking with TMotion, we are capable of expanding the interaction space to both above and behind device. On the other hand, TMotion delivers a wide range of interaction types such as hovering, tracing, and pointing. We categorize the provided interactions into continuous spatial tracking and discrete spatial zoning. We consider the spatial tracking as a continuous relationship tailored to the user intents expressed by natural motions. We characterize the spatial zoning as a dissection of physical volume around the mobile device or the real object into several zones to embed discrete information.

In above device interaction space, we demonstrate the spatial tracking feature with an example that associates user movement with the measurement of object's dimensions. The multi-level menu interface shows how we use above device spatial zones to embed discrete information. For behind device, we leverage the back camera on the smartphone, and construct applications in AR environment. Through this set up, we show direct manipulation and registration of digital

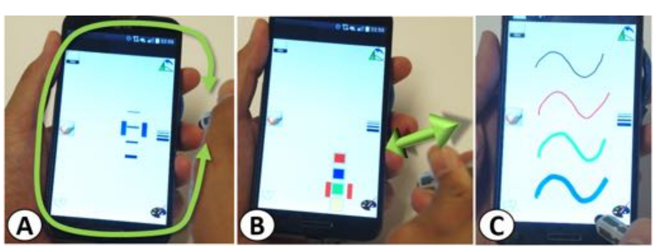

Figure 10. TMotion enables a mid-air multi-level menu control offering (A) hovering around the device to open option lists and (B) depth control and tapping for option selection (C) in a drawing application.

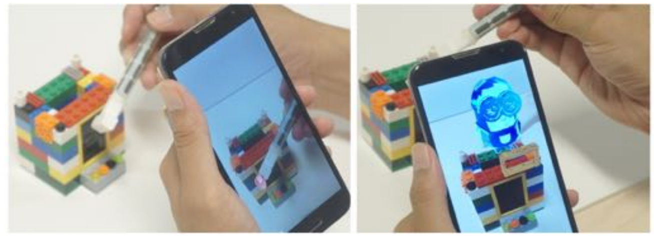

Figure 11. TMotion is aligned with virtual model in the augmented scene (Left). The system enables manipulating virtual blocks with respect to the physical object (Right).

contents within the augmented scene using continuous and discrete interactions respectively.

Above Device Interaction

Spatial tangible measurements: With a spatial tracking above the device, application designers are encouraged to utilize the mid-air interaction space. As described in SPATA [29], the measurement is one of a key element for fabrication-aware context, especially for designers. Here, we develop an application which measures dimensions of real objects. First, users take picture of the target object. Then, users pre-annotate the measurements that will be taken. Subsequently, users place the stylus tip on the interesting points and tap pen body to complete the measurements. For length and angle measurements, 2-points and 3-points selection are required respectively. Upon completing the physical measurement, results will be displayed on the pre-selected annotation label (Figure 9). This illustrates TMotion's capability to achieve the user-guided spatial tracking above the device.

Multi-level menu interface: Previously, single menu control using around device interaction has been demonstrated based on 2D tracking [15, 19]. Using 3D position information offered by TMotion, we implement richer interactions through 3D spatial zones formed around the mobile device. We constructed a drawing application embedded with a mid-air controlled multi-level menu interface. While hovering around the displayed icons, user pops up a first-level menu. Then, the user moves along the z-axis to hover the option list and taps to confirm selection. This showcases richer interactions using discrete spatial zones around the mobile device.

Behind Device Interaction

In our AR applications, we use Vuforia™ SDK for tracking in physical environment. In both demos, pre-built LEGO

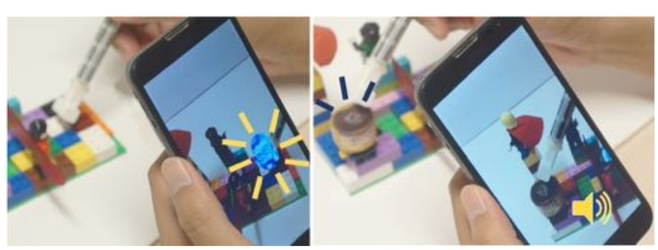

Figure 12. TMotion interacts with the spatially embedded digital contents around the real objects such as discovering hidden virtual character (Left) and playing sounds for different characters (Right).

blocks are used as world frame reference. The natural feature points of the LEGO blocks are first captured and stored for object tracking and recognition purpose. Furthermore, we align the physical pen tip with corresponding virtual contents within an augmented scene.

In-situ building blocks: The early tangible AR manipluation which is based on monocular vision tracking suffers from occlusion and bulky size of the marker [32]. On the other hand, TMotion enables a low profile 3D input device in mobile AR application by providing full 3D tracking capability. Here, we apply TMotion to manipulate the virtual contents directly. Users place and drop virtual models onto the existing LEGO construction within the augmented scene. The virtual creations are superimposed onto the designated locations. Then, users conduct visual inspections from different points of view by moving the mobile device. This example showcases the use of continuous interactions behind the device.

Digital contents overlay: The mobile AR setup also suffers from the limited alternatives to interact with the physical environment. Vuforia SDK provides a virtual button solution which is triggered by blocking the line-of-sight view. Such solution requires users to block the printed buttons on a marker sheet to trigger them. However, 3D tracking using TMotion allows us utilizing the discrete spatial zoning feature. We successfully embed the virtual contents including sounds and virtual characters into the dissected space around the physical LEGO blocks. To access the contents, user can hover or tap in the specific regions in the physical world. This demonstrates TMotion's capability of providing discrete interactions behind the device.

DISCUSSION

In this work, we show that TMotion achieves a real-time 3D position tracking with a deeper understanding of user intents in 3D mobile space. Our work represents human's natural motion with physical input device as an embedded 3D interaction. Demonstrated applications show a potential to offer new interaction metaphors which cannot be provided by previous 2D tracking or gesture based discrete inputs. Here, we discuss design implications, limitations and future work.

Coarse Interaction Strata for Discrete Input: We observe that the performance of targeting in the mid-air using a physical input device becomes worse under 20mm layer thickness. Multiple factors other than the system performance comes into play such as fatigue from the users during the mid-air interaction. This implies that even if the system supports better accuracy, the users still have limited discrete controllability above the device. Aligned with previous study [28], our finding also suggests to use coarse interaction strata for above device interaction with 3D mobile input to provide an acceptable discrete input controllability.

3D Mobile Input as Spatial Tangible Interaction: For spatial tangible interaction, the tracking accuracy during physical interaction decides the overall performance. From our task evaluation with users, we noticed that the tracking accuracy with the physical object improved from experimental results due to the user's tendency of interacting near the mobile device. We presume users prefer the near-surface interaction in order to maintain the visibility of the mobile screen. This implies that the 3D mobile input offered by TMotion has a potential to provide spatial inputs for tangible interaction.

Real-time Registration in Augmented Scene: Registration of the virtual contents to the physical input device in the augmented scene is particularly important to seamlessly connect virtual and physical worlds. In this work, we successfully register the virtual and the physical pen tips by translating the tracked pen tip from the magnetometer's frame to camera frame and scaling the interaction volume to fit into the video scene. Furthermore, we use the camera's pose estimation to superimpose the virtual contents to the physical environment. Through examples, we successfully showcase using the physical 3D input device freely manipulates virtual contents in AR environment. This implies that TMotion could potentially serve as an interaction medium to support upcoming mobile AR interface.

There are several limitations to the current version of TMotion. First, our approach requires subsequent maintenance of the device's orientation after an initial calibration. We plan to solve this issue with orientation estimation using either extended Kalman filter or magnetic dip angle detection where both methods work even under magnetic perturbation [30].

The interaction volume is still limited under 100mm above and behind the device. Simply increasing the strength of the magnet does not enlarge the interaction space proportionally. We tested our prototype with a stronger magnet (ϕ = 6mm, 15T), but it created a large saturation near the sensor due to the strong magnetic field and lost the dipole characteristics from the length of the magnet. However, this would be remedied by using upcoming magnetometers that have higher magnetic field sensing resolution and range.

Future work will include further expansion of applications into both AR and VR fields. We are in process of enhancing the prototype to be compatible with different size of mobile devices including tablet and smartwatch. Extensive user studies with real applications using proposed technique are also within our interest. These works will explore how users perform and perceive 3D mobile input for upcoming interfaces.

CONCLUSION

In this paper, we present TMotion, an embedded 3D mobile input using magnetic sensing technique. With the known orientations from 9DOF-IMU, we explicitly solve the position of the embedded magnet through numerical solver. In our experiments, we have shown that TMotion achieves a real-time and accurate 3D tracking with an existing mobile device. We also verify that TMotion maintains tracking and targeting accuracy with real users. Example applications showcase the continuous/discrete interactions in expanded spaces. As 3D mobile interfaces develop, the needs for better method to handle and exploit richer user inputs also increase. We demonstrate that TMotion potentially fulfills these requirements by presenting a real-time 3D mobile input.

ACKNOWLEDGMENT

This work was partially supported by the NSF under grants CMMI-EDI 1235232 and IGERT 1144842. Any opinions, findings, and conclusions or recommendations expressed in this material are those of the authors and do not necessarily reflect the views or opinions of the funding agency.

REFERENCES

1. Michelle Annett, Fraser Anderson, Walter F Bischof, and Anoop Gupta. 2014. The pen is mightier: understanding stylus behaviour while inking on tablets. In *Proceedings of the 2014 Graphics Interface Conference (GI'14)*. 193–200.
2. Daniel Ashbrook, Patrick Baudisch, and Sean White. 2011. Nenya: subtle and eyes-free mobile input with a magnetically-tracked finger ring. In *Proceedings of the ACM SIGCHI Conference on Human factors in computing systems (CHI'11)*. 2043–2046.
3. Ravin Balakrishnan and I Scott MacKenzie. 1997. Performance differences in the fingers, wrist, and forearm in computer input control. In *Proceedings of the SIGCHI Conference on Human Factors in Computing Systems (CHI'97)*. 303–310.
4. Andrea Bianchi and Ian Oakley. 2015. MagnID: Tracking Multiple Magnetic Tokens. In *Proceedings of the Ninth International Conference on Tangible, Embedded, and Embodied Interaction (TEI'15)*. 61–68.
5. Paul Bouchier. 2013. Razor 9DOF AHRS. (2013). Retrieved August 1, 2015 from `https://github.com/ptrbrtz/razor-9dof-ahrs`.
6. Alex Butler, Shahram Izadi, and Steve Hodges. 2008. SideSight: multi-touch interaction around small devices. In *Proceedings of the 21st annual ACM symposium on User interface software and technology (UIST'08)*. 201–204.
7. Liwei Chan, Rong-Hao Liang, Ming-Chang Tsai, Kai-Yin Cheng, Chao-Huai Su, Mike Y Chen, Wen-Huang Cheng, and Bing-Yu Chen. 2013. Fingerpad: private and subtle interaction using fingertips. In *Proceedings of the 26th annual ACM symposium on User interface software and technology (UIST'13)*. 255–260.
8. Ke-Yu Chen, Kent Lyons, Sean White, and Shwetak Patel. 2013. uTrack: 3D input using two magnetic sensors. In *Proceedings of the 26th annual ACM symposium on User interface software and technology (UIST'13)*. 237–244.
9. Xiang'Anthony' Chen, Julia Schwarz, Chris Harrison, Jennifer Mankoff, and Scott E Hudson. 2014. Air+ touch: interweaving touch & in-air gestures. In *Proceedings of the 27th annual ACM symposium on User interface software and technology (UIST'14)*. 519–525.
10. Google. 2013. Cardboard. (2013). Retrieved August 1, 2015 from `https://www.google.com/get/cardboard`.
11. Xinying Han, Hiroaki Seki, Yoshitsugu Kamiya, and Masatoshi Hikizu. 2009. Wearable handwriting input device using magnetic field: Geomagnetism cancellation in position calculation. *Precision engineering* 33, 1 (2009), 37–43.
12. Chris Hand. 1997. A survey of 3D interaction techniques. In *Computer graphics forum*, Vol. 16. Wiley Online Library, 269–281.
13. Chris Harrison and Scott E Hudson. 2009. Abracadabra: wireless, high-precision, and unpowered finger input for very small mobile devices. In *Proceedings of the 22nd annual ACM symposium on User interface software and technology (UIST'09)*. 121–124.
14. Ken Hinckley, Michel Pahud, Hrvoje Benko, Pourang Irani, François Guimbretière, Marcel Gavriliu, Xiang 'Anthony' Chen, Fabrice Matulic, William Buxton, and Andrew Wilson. 2014. Sensing Techniques for Tablet+Stylus Interaction. In *Proceedings of the 27th annual ACM symposium on User interface software and technology (UIST'14)*. 605–614.
15. Sungjae Hwang, Andrea Bianchi, Myungwook Ahn, and Kwangyun Wohn. 2013. MagPen: magnetically driven pen interactions on and around conventional smartphones. In *Proceedings of the 15th International Conference on Human-Computer Interaction with Mobile Devices and Services (MobileHCI'13)*. 412–415.
16. Brett Jones, Rajinder Sodhi, David Forsyth, Brian Bailey, and Giuliano Maciocci. 2012. Around device interaction for multiscale navigation. In *Proceedings of the 14th international conference on Human computer interaction with mobile devices and services (MobileHCI'12)*. 83–92.
17. Hamed Ketabdar, Mehran Roshandel, and Kamer Ali Yüksel. 2010. MagiWrite: towards touchless digit entry using 3D space around mobile devices. In *Proceedings of the 12th International Conference on Human-Computer Interaction with Mobile Devices and Services (MobileHCI'10)*. 443–446.
18. Igor Khalfin and Herbert S Jones Jr. 2002. Electromagnetic position and orientation tracking system with distortion compensation employing wireless sensors. (April 2 2002). U.S. Patent 6,369,564.
19. Rong-Hao Liang, Kai-Yin Cheng, Chao-Huai Su, Chien-Ting Weng, Bing-Yu Chen, and De-Nian Yang. 2012. GaussSense: attachable stylus sensing using magnetic sensor grid. In *Proceedings of the 25th annual ACM symposium on User interface software and technology (UIST'12)*. 319–326.
20. Microsoft. 2012. Surface. (2012). Retrieved August 1, 2015 from `https://www.microsoft.com/surface`.
21. NVIDIA. 2013. SHIELD. (2013). Retrieved August 1, 2015 from `http://shield.nvidia.com/tablet`.

22. Qualcomm. 2012. Vuforia. (2012). Retrieved August 1, 2015 from `https://www.qualcomm.com/products/vuforia`.
23. Amir Rubin and Jeffrey Peter Bellinghausen. 2013. Passive and active video game controllers with magnetic position sensing. (Dec. 31 2013). U.S. Patent 8,616,974.
24. Samsung. 2014. Galaxy Note Edge. (2014). Retrieved August 1, 2015 from `http://www.samsung.com/global/microsite/galaxynoteedge`.
25. Udo Schultheis, Jason Jerald, Fernando Toledo, Arun Yoganandan, and Paul Mlyniec. 2012. Comparison of a two-handed interface to a wand interface and a mouse interface for fundamental 3D tasks. In *2012 IEEE Symposium on 3D User Interfaces (3DUI)*. 117–124.
26. Hyunyoung Song, Hrvoje Benko, Francois Guimbretiere, Shahram Izadi, Xiang Cao, and Ken Hinckley. 2011. Grips and Gestures on a Multi-touch Pen. In *Proceedings of the SIGCHI Conference on Human Factors in Computing Systems (CHI'11)*. 1323–1332.
27. Jie Song, Gábor Sörös, Fabrizio Pece, Sean Ryan Fanello, Shahram Izadi, Cem Keskin, and Otmar Hilliges. 2014. In-air gestures around unmodified mobile devices. In *Proceedings of the 27th annual ACM symposium on User interface software and technology (UIST'14)*. 319–329.
28. Chat Wacharamanotham, Kashyap Todi, Marty Pye, and Jan Borchers. 2014. Understanding finger input above desktop devices. In *Proceedings of the SIGCHI Conference on Human Factors in Computing Systems (CHI'14)*. 1083–1092.
29. Christian Weichel, Jason Alexander, Abhijit Karnik, and Hans Gellersen. 2015. SPATA: Spatio-tangible tools for fabrication-aware design. In *Proceedings of the Ninth International Conference on Tangible, Embedded, and Embodied Interaction (TEI'15)*. 189–196.
30. Nagesh Yadav and Chris Bleakley. 2014. Accurate Orientation Estimation Using AHRS under Conditions of Magnetic Distortion. *Sensors* 14, 11 (2014), 20008–20024.
31. Kamer Ali Yuksel, Ipek Baz, and Haluk Ozduman. 2015. Using Electromagnetic Input for Multi-User or Two-Handed Spatial Gestural Interaction based on the Digital Compass. In *Proceedings of the 17th international conference on Human computer interaction with mobile devices and services (MobileHCI'15)*. 420–426.
32. Feng Zhou, Henry Been-Lirn Duh, and Mark Billinghurst. 2008. Trends in augmented reality tracking, interaction and display: A review of ten years of ISMAR. In *Proceedings of the 7th IEEE/ACM International Symposium on Mixed and Augmented Reality (ISMAR'08)*. 193–202.